

Positrons at JLab Advancing Nuclear Science in Hall B

Volker D. Burkert^{1,a)}

¹Jefferson Laboratory, 12000 Jefferson Avenue, Newport News, Virginia, 23606

^{a)}Corresponding author: burkert@jlab.org

Abstract. In this talk I address two high impact physics programs that require the use of polarized and unpolarized positron beams in addition to using electron beams of the same energy. First, I address what will be gained from using positron beams in addition to electron beams in the extraction of the Compton Form Factors (CFFs) and generalized parton distributions (GPDs) from Deeply Virtual Compton Scattering (DVCS) on a proton target. As a second high impact science program I discuss an experimental scenario using unpolarized positrons to measure elastic scattering on protons in an effort to determine definitively the 2-photon exchange contributions in order to resolve a longstanding discrepancy in the determination of the proton's electric and magnetic form factors.

INTRODUCTION

The challenge of understanding nucleon electromagnetic structure still continues after six decades of experimental scrutiny. From the initial measurements of elastic form factors to the accurate determination of parton distributions through deep inelastic scattering, the experiments have increased in statistical and systematic accuracy. During the past two decades it was realized that the parton distribution functions represent special cases of a more general, much more powerful, way to characterize the structure of the nucleon, the generalized parton distributions (GPDs) (see [1, 2] for reviews).

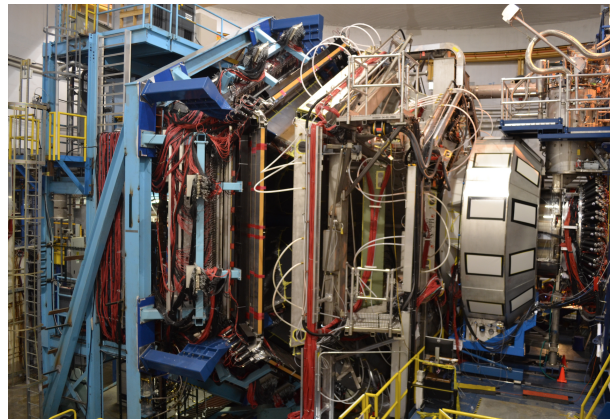


FIGURE 1. The CLAS12 detector in Hall B. The detector was designed for inclusive, semi-inclusive, as well as exclusive processes such as DVCS. The construction and commissioning of the detector system was completed recently. CLAS12 is part of the DOE funded energy upgrade of the Jefferson Lab CEBAF accelerator from 6 GeV to 12 GeV, and may play an important role in programs that make use of positron beams at Jefferson Lab.

The GPDs are the Wigner quantum phase space distribution of quarks in the nucleon describing the simultaneous distribution of particles with respect to both position and momentum in a quantum-mechanical system. In addition to the information about the spatial density and momentum density, these functions reveal the correlation of the spatial

and momentum distributions, *i.e.* how the spatial shape of the nucleon changes when probing quarks of different momentum fraction of the nucleon.

The concept of GPDs has led to completely new methods of “spatial imaging” of the nucleon in the form of (2+1)-dimensional tomographic images, with 2 spatial dimensions and 1 dimension in momentum [3, 4, 5]. The second moments of GPDs are related to form factors that allow us to quantify how the orbital motion of quarks in the nucleon contributes to the nucleon spin, and how the quark masses and the forces on quarks are distributed in transverse space, a question of crucial importance for our understanding of the dynamics underlying nucleon structure and the forces leading to color confinement.

The four leading twist GPDs H , \tilde{H} , E , and \tilde{E} , depend on the 3 variable x , ξ , and t , where x is the longitudinal momentum fraction of the struck quark, ξ is the longitudinal momentum transfer to the quark ($\xi \approx x_B/(2 - x_B)$), and t is the invariant 4-momentum transfer to the proton. The mapping of the nucleon GPDs, and a detailed understanding of the spatial quark and gluon structure of the nucleon, have been widely recognized as key objectives of nuclear physics of the next decades. This requires a comprehensive program, combining results of measurements of a variety of processes in electron–nucleon scattering with structural information obtained from theoretical studies, as well as with expected results from future lattice QCD simulations. The CLAS12 detector, shown in Fig. 1, has recently been completed and has begun the experimental science program in the 12 GeV era Jefferson Lab.

ACCESSING GPD IN DVCS

The most direct way of accessing GPDs at lower energies is through the measurement of Deeply Virtual Compton Scattering (DVCS) in a kinematical domain where the so-called handbag diagram shown in Fig. 2 makes the dominant contributions. However, in DVCS as in other deeply virtual reactions, the GPDs do not appear directly in the cross section, but in convolution integrals, e.g.

$$\int_{-1}^{+1} \frac{H^q(x, \xi, t) dx}{x - \xi + i\epsilon} = \int_{-1}^{+1} \frac{H^q(x, \xi, t) dx}{x - \xi} + i\pi H^q(\xi, \xi, t), \quad (1)$$

where the first term on the r.h.s. corresponds to the real part and the second term to the imaginary part of the scattering amplitude. The superscript q indicates that GPDs depend on the quark flavor. From the above expression it is obvious that GPDs, in general, can not be accessed directly in measurements. However, in some kinematical regions the Bethe-Heitler (BH) process where high energy photons are emitted from the incoming and scattered electrons, can be important. Since the BH amplitude is purely real, the interference with the DVCS amplitude isolates the imaginary part of the DVCS amplitude. The interference of the two processes offers the unique possibility to determine GPDs directly at the singular kinematics $x = \xi$. At other kinematical regions a deconvolution of the cross section is required to determine the kinematic dependencies of the GPDs. It is therefore important to obtain all possible independent information that will aid in extracting information on GPDs. The interference terms for polarized beam I_{LU} , longitudinally polarized target I_{UL} , transversely (in scattering plane) polarized target I_{UT} , and perpendicularly (to scattering plane) polarized target I_{UP} are given by the expressions:

$$I_{LU} \sim \sqrt{\tau'} [F_1 H + \xi(F_1 + F_2) \tilde{H} + \tau F_2 E] \quad (2)$$

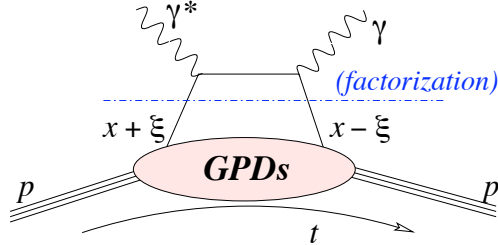


FIGURE 2. Leading order contributions to the production of high energy single photons from protons. The DVCS handbag diagram contains the information on the unknown GPDs.

$$I_{UL} \sim \sqrt{\tau'} [F_1 \tilde{H} + \xi(F_1 + F_2)H + (\tau F_2 - \xi F_1)\xi \tilde{E}] \quad (3)$$

$$I_{UP} \sim \tau [F_2 H - F_1 E + \xi(F_1 + F_2)\xi \tilde{E}] \quad (4)$$

$$I_{UT} \sim \tau [F_2 \tilde{H} + \xi(F_1 + F_2)E - (F_1 + \xi F_2)\xi \tilde{E}] \quad (5)$$

where $\tau = -t/4M^2$, $\tau' = (t_0 - t)/4M^2$. By measuring all 4 combinations of interference terms one can separate all 4 leading twist GPDs at the specific kinematics $x = \xi$. Experiments at JLab using 4 to 6 GeV electron beams have been carried out with polarized beams [6, 7, 8, 9, 10] and with longitudinal target [11, 12, 13], showing the feasibility of such measurements at relatively low beam energies, and their sensitivity to the GPDs. Techniques of how to extract GPDs from existing DVCS data and what has been learned about GPDs can be found in [14, 15]. In the following sections we discuss what information may be gained by employing both electron and positron beams in deeply virtual photon production.

Differential cross section for polarized electrons and positrons (leptons)

The structure of the differential cross section for polarized beam and unpolarized target is given by:

$$\sigma_{\bar{e}p \rightarrow e\gamma p} = \sigma_{BH} + e_\ell \sigma_{INT} + P_\ell e_\ell \tilde{\sigma}_{INT} + \sigma_{VCS} + P_\ell \tilde{\sigma}_{VCS} \quad (6)$$

where σ is even in azimuthal angle ϕ , and $\tilde{\sigma}$ is odd in ϕ . The interference terms $\sigma_{INT} \sim \text{Re}A_{\gamma^*N \rightarrow \gamma N}$ and $\tilde{\sigma}_{INT} \sim \text{Im}A_{\gamma^*N \rightarrow \gamma N}$ are the real and imaginary parts, respectively of the Compton amplitude. Using polarized electrons the combination $-\tilde{\sigma}_{INT} + \tilde{\sigma}_{VCS}$ can be determined by taking the difference of the beam helicities. The electron-positron charge difference for unpolarized beams determines σ_{INT} . For fixed beam polarization and taking the electron-positron difference one can extract the combination $P_\ell \tilde{\sigma}_{INT} + \sigma_{INT}$. If only a polarized electron beam is available one can separate $\tilde{\sigma}_{INT}$ from $\tilde{\sigma}_{VCS}$ using the Rosenbluth technique [16]. This requires measurements at two significantly different beam energies which reduces the kinematical coverage that can be achieved with this method. With polarized electrons and polarized positrons both σ_{INT} can be determined and $\tilde{\sigma}_{INT}$ can be separated from $\tilde{\sigma}_{VCS}$ in the full kinematic range available at the maximum beam energy.

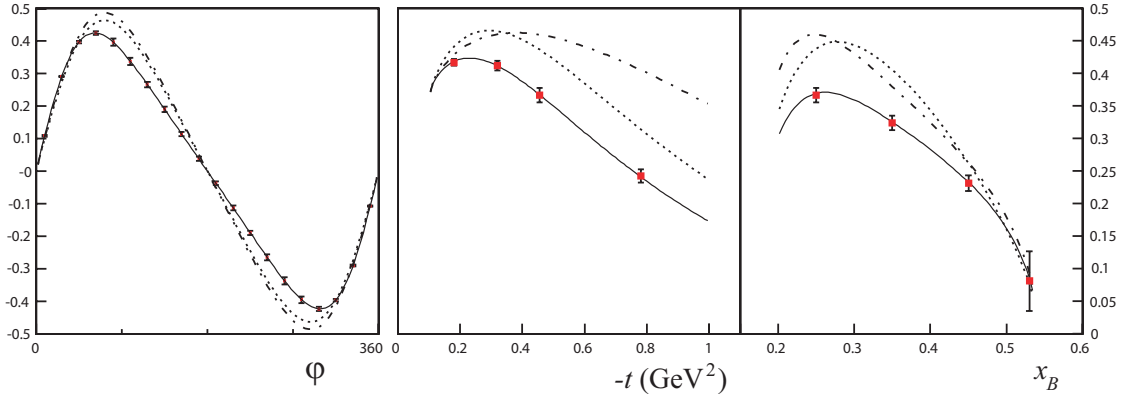


FIGURE 3. The beam spin asymmetry showing the DVCS-BH interference for 11 GeV beam energy [17]. Left panel: $x = 0.2$, $Q^2 = 3.3 \text{ GeV}^2$, $-t = 0.45 \text{ GeV}^2$. Middle and right panels: $\phi = 90^\circ$, other parameters same as in left panel. Many other bins will be measured simultaneously. The curves represent various parameterizations within the VGG model [18]. Projected uncertainties are statistical.

Differential cross section for polarized proton target

The structure of the differential cross section for polarized beam and polarized target contains the polarized beam term of the previous section and an additional term related to the target polarization [19, 20]:

$$\sigma_{\bar{e}\vec{p} \rightarrow e\gamma p} = \sigma_{\bar{e}p \rightarrow e\gamma p} + T [P_\ell \Delta \sigma_{BH} + e_\ell \Delta \tilde{\sigma}_{INT} + P_\ell e_\ell \Delta \sigma_{INT} + \Delta \tilde{\sigma}_{VCS} + P_\ell \Delta \sigma_{VCS}] \quad (7)$$

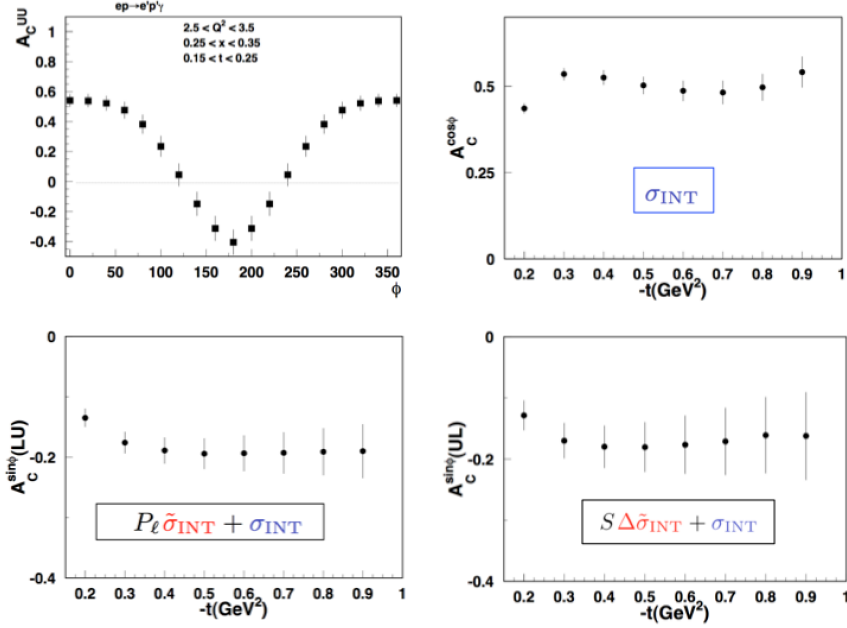


FIGURE 4. Electron-positron DVCS charge asymmetries: Top-left: Azimuthal dependence of the charge asymmetry for positron and electron beam at 11 GeV beam. Top-right: Moment in $\cos(\phi)$ of the charge asymmetry versus momentum transfer t to the proton. Bottom-left: Charge asymmetries for polarized electron and positron beams at fixed polarization (LU). Bottom right: Charge asymmetry for longitudinally polarized protons at fixed polarization (UL). The error bars are estimated for a 1000 hrs run with positron beam and luminosity $L = 2 \times 10^{34} \text{ cm}^{-2}\text{sec}^{-1}$ at a beam polarization $P = 0.6$. Electron luminosity $L = 10 \times 10^{34} \text{ cm}^{-2}\text{sec}^{-1}$, and electron beam polarization $P = 0.8$. The error bars are statistical for a single bin in Q^2 , x , and t as shown in the top-left panel. Other bins are measured simultaneously.

where the target polarization T can be longitudinal or transverse. If only unpolarized electrons are available, the combination $-\Delta\tilde{\sigma}_{INT} + \Delta\tilde{\sigma}_{VCS}$ can be measured from the differences in the target polarizations. If unpolarized electrons and unpolarized positrons are available the combination $T\Delta\tilde{\sigma}_{INT} + \sigma_{INT}$ can be determined at fixed target polarization. With both polarized electron and polarized positron beams, the combination $T\Delta\tilde{\sigma}_{INT} + TP_t\Delta\sigma_{INT} + P_t\tilde{\sigma}_{INT} + \sigma_{INT}$ can be measured at fixed target polarization. Availability of both polarized electron and polarized positron beams thus allows the separation of all contributing terms. If only polarized electron beams are available a Rosenbluth separation with different beam energies can separate the term $\Delta\tilde{\sigma}_{INT}$ from $\Delta\tilde{\sigma}_{VCS}$, again in a much more limited kinematical range and with likely larger systematic uncertainties. The important interference term $\Delta\sigma_{INT}$ can only be determined using the combination of polarized electron and polarized positron beams.

Estimates of charge asymmetries for different lepton charges

For quantitative estimates of the charge differences in the cross sections we use the acceptance and luminosity achievable with CLAS12 as basis for measuring the process $ep \rightarrow eyp$ at different beam and target conditions. A 10 cm long liquid hydrogen is assumed with an electron current of 40nA, corresponding to an operating luminosity of $10^{35} \text{ cm}^{-2}\text{sec}^{-1}$. For the positron beam a 5 times lower beam current of 8nA is assumed. In either case 1000 hours of beam time is used for the rate projections. For quantitative estimates of the cross sections the dual model [21, 22] is used. It incorporates parameterizations of the GPDs H and E . As shown in Fig. 4, effects coming from the charge asymmetry can be large. In case of unpolarized beam and unpolarized target the cross section for electron scattering has only a small dependence on azimuthal angle ϕ , while the corresponding positron cross section has a large ϕ modulation. The difference is directly related to the term σ_{INT} in equation (6).

Experimental Setup for DVCS Experiments

Figure 5 shows generically how the electron-proton and the positron-proton DVCS experiments could be configured. Electrons and positrons would be detected in the forward detection system of CLAS12. However, for the positron run the Torus magnet would have the reversed polarity so that positron trajectories would look identical to the electron trajectories in the electron-proton experiment, and limit systematic effects in acceptances. The recoil proton in both cases would be detected in the Central Detector at the same solenoid magnet polarity, also eliminating most systematic effects in the acceptances. However, there is a remaining systematic difference in the two configuration, as the forward scattered electron/positron would experience different transverse field components in the solenoid, which will cause the opposite azimuthal motion in ϕ in the forward detector. A good understanding of the acceptances in both cases is therefore important. The high-energy photon is, of course, not affected by the magnetic field configuration.

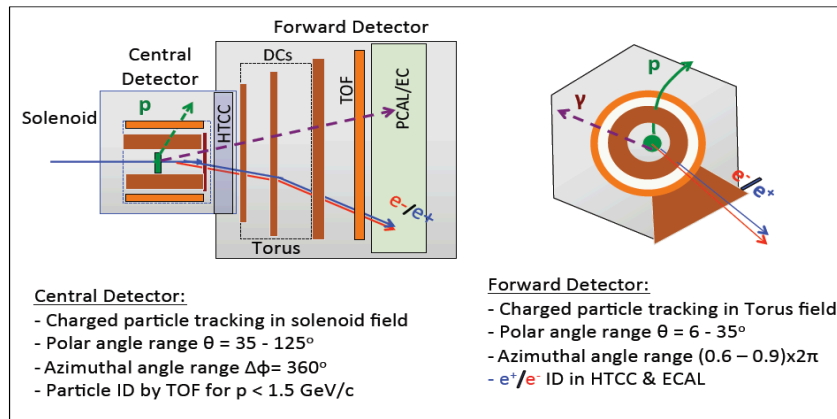


FIGURE 5. CLAS12 configuration for the two electron and positron experiments (generic). The central detector will detect the protons, and the bending in the magnetic solenoid field will be identical for the same kinematics. The electron and the positron, as well as the high-energy DVCS photon will be detected in the forward detector part. The electron and positron will be deflected in the Torus magnetic field in the same way as the Torus field direction will be opposite in the two experiments. The deflection in ϕ due to the solenoid fringe field will be of same magnitude $\Delta\phi$ but opposite in direction. The systematic of this shift can be controlled by doing the same experiment with opposite solenoid field directions that would result in the sign change of the $\Delta\phi$.

In the next section we discuss a possible solution to the, so-far, not conclusive experimental studies of two-photon effects in elastic electron-proton scattering and their effect on the ratio of electric to magnetic form factors G_E/G_M versus Q^2 .

2-PHOTON EFFECTS IN ELASTIC SCATTERING OFF PROTONS

In the electromagnetic physics community it is well known that two experimental approaches, the Rosenbluth separation and the beam polarization transfer approach results in conflicting values for the G_E/G_M ratio when plotted as a function of Q^2 . The results of the different experimental methods are compiled in Fig. 6. The trends of the two data sets are inconsistent with each other, although there is a large spread in the Rosenbluth data samples. The latter seem to be more consistent with near Q^2 -independent behavior, while the polarization data have a strong downward behavior with Q^2 . Furthermore, the uncertainties in the former are much larger and within the individual data sets there seem to be discrepancies as well. The difference of the two methods may be attributed to 2-photon exchange effects, which are expected to be much more important in the cross section subtraction method than in the polarization transfer method.

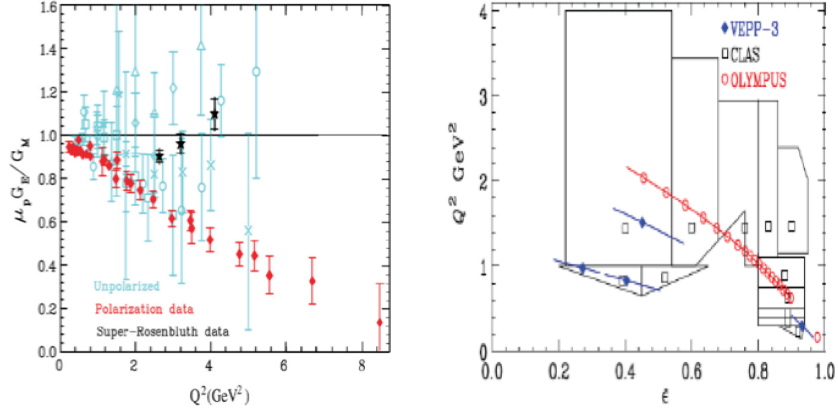


FIGURE 6. Left panel: The ratio of the proton electric and magnetic form factors G_E/G_M . The cyan markers are results of experiments based on the Rosenbluth method. The red markers are from JLab Hall A experiments. Right panel: Kinematics covered by the three recent experiments to measure the 2-photon exchange contribution to the elastic ep cross section. Both figures are taken from a recent review article [27].

Recent efforts to quantify 2-photon exchange contributions

It is obviously important to resolve the discrepancy with experiments that have sensitivity to 2-photon contributions. The most straightforward process to evaluate 2-photon contribution is the measurement of the ratio of elastic e^+p/e^-p scattering, which in leading order is given by the expression: $R_{2\gamma} = 1 - 2\delta_{\gamma\gamma}$. Several experiments have recently been carried out to measure the 2-photon exchange contribution in elastic scattering: the VEPP-3 experiment at Novosibirsk [23], the CLAS experiment at Jefferson Lab [24, 25], and the Olympus experiment at DESY [26]. The kinematic reach of each experiment is shown in the right panel of Fig. 6. The kinematic coverage is much smaller in these experiments $Q^2 < 2 \text{ GeV}^2$, and $\epsilon > 0.5$, where the 2-photon effects are expected to be small, and systematics of the measurements must be extremely well controlled. The combined evaluation of all three experiments led the authors of the review article Ref. [27] to the conclusion that the results of the experiments are inconsistent with the $\delta_{\gamma\gamma} = 0$ hypothesis at 99.5% confidence. At the same time, they state that "the results of these experiments are by no means definitive", and "there is a clear need for similar experiments at larger Q^2 and at $\epsilon < 0.5$."

Conclusions From Previous Experiments

In the following I discuss a possible experiment with CLAS12 at Jefferson Lab that may be able to remedy the shortcomings of the previous measurements. What are these shortcomings?

- Kinematics coverage in Q^2 and in ϵ are mostly where 2-photon effects are expected to be small
- Systematic uncertainties are marginal in some cases
- Higher Q^2 and small ϵ corresponding to high energy and large electron scattering angles were out of reach

Can we do better with a setup using the modified CLAS12 detector? To address this question we begin with the close to ideal kinematic coverage that this setup provides. Figure 7 shows the angle coverage for both the electron (left) and for the proton (right). There is a one-to-one correlation between the electron scattering angle and the proton recoil angle. For the kinematics of interest, say $\epsilon < 0.6$ and $Q^2 > 2 \text{ GeV}^2$ for the chosen beam energies from 2.2 to 6.6 GeV, nearly all of the electron scattering angles fall into a polar angle range from 40° to 125° , and corresponding to the proton polar angle range from 8° to 35° . While these kinematics are most suitable for accessing the 2-photon exchange contributions, the setup will be able to also measure the reversed kinematics with the electrons at forward angle and the protons at large polar angles. This is in fact the standard CLAS12 configuration of DVCS and most other experiments, however it will not cover the kinematics with highest sensitivity to the 2-photon exchange contributions.

Figure 8 shows the expected elastic scattering rates covering the ranges of highest interest, with $\epsilon < 0.6$ and $Q^2 = 2 - 10 \text{ GeV}^2$. Sufficiently high statistics of $\sigma_N/N < 1\%$ can be achieved within 10 hrs for the lowest energy and within 1000 hrs for the highest energy, to cover the full range in kinematics. Note that all kinematic bins will be measured simultaneously at a given energy, and the shown rates are for the individual bins in $Q^2 - \epsilon$ space.

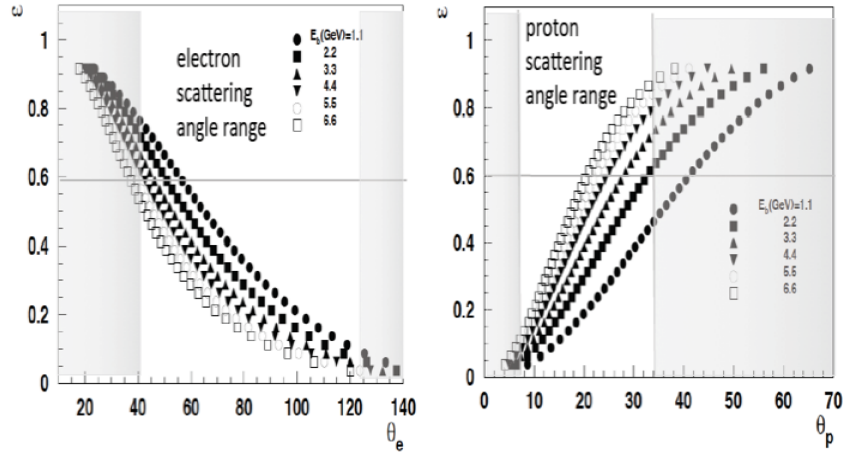


FIGURE 7. Polar angle and ϵ coverage for electron detection (left) and for proton detection (right).

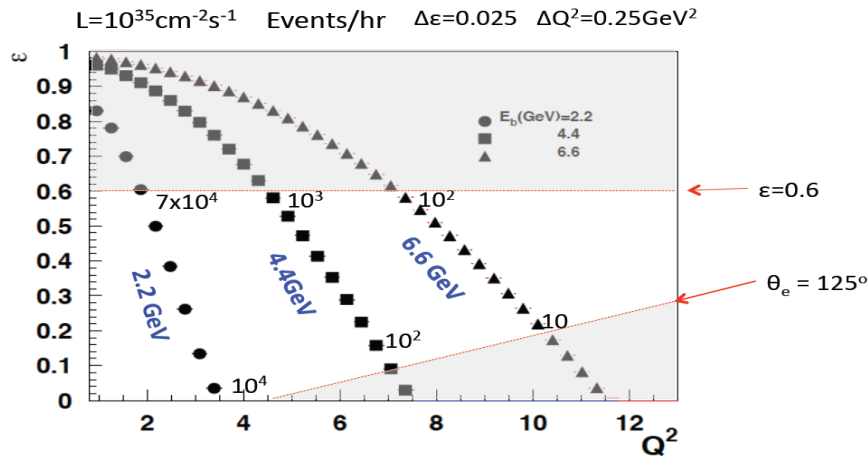


FIGURE 8. Estimated elastic event rates per hour for selected standard CEBAF beam energies of 2.2, 4.4, 6.6 GeV in the $\epsilon - Q^2$ plane. Rates are given only for the lowest and highest Q^2 bin.

A New Experimental Setup - Kinematic Coverage and Rate Estimates

In order to achieve the desired reach in Q^2 and ϵ the CLAS12 detection system has to be used with reversed detection capabilities for electrons. The main modification will involve replacing the current Central Neutron Detector (CND) with a central electromagnetic calorimeter (CEC). The CEC will not need very good energy or angle resolution (both are provided by the tracking detectors) but will be used for trigger purposes and to aid in electron/pion separation. The over constrained kinematics of measured scattered electrons and recoil protons should be sufficient to select the elastic kinematics and eliminated any background (this will have to be demonstrated by detailed simulations).

For the rate estimates and the kinematical coverage we have made a number of assumptions that are not overly stringent:

- Positron beam currents (unpolarized): $I_{e^+} \approx 60$ nA.
- Beam profile: $\sigma_x, \sigma_y < 0.4$ mm.
- Polarization: not required, so phase space at the source maybe chosen for optimized yield and beam parameters.
- Obtain the electron beam from the same source as the positrons to keep systematic under control.
- Switching from e^+ to e^- operation should be doable in reasonable time frame (< 1 day) to keep machine stable, and systematics under control.

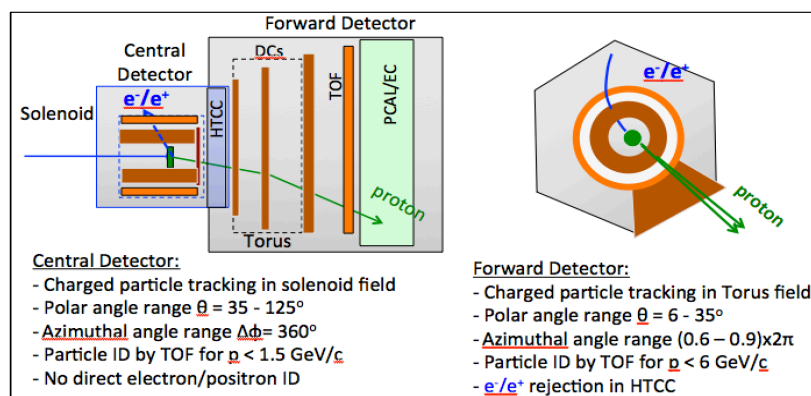


FIGURE 9. CLAS12 configuration for the elastic e^-p/e^+p scattering experiment (generic). The central detector will detect the electron/positrons, and bending in the solenoid magnetic field will be identical for the same kinematics. The proton will be detected in the forward detector part. The Torus field direction will be the same in both cases. The deflection in ϕ due to the solenoid fringe field will be of same in magnitude of $\Delta\phi$ but opposite in direction. The systematic of this shift can be controlled by doing the same experiment with opposite solenoid field directions that would result in the sign change of the $\Delta\phi$.

- Operate experiment with 5cm liquid H_2 target and luminosity of $0.8 \times 10^{35} \text{ cm}^2\text{sec}^{-1}$
- Use the CLAS12 Central Detector for lepton (e^+/e^-) detection at $\Theta_l = 40 - 125^\circ$.
- Use CLAS12 Forward Detector for proton detection at $\Theta_p = 7^\circ - 35^\circ$

The CLAS12 configuration suitable for this experiment is shown in Fig. 9.

SUMMARY

Availability of a 11 GeV positron beam at JLab can significantly enhance the experimental program using the CLAS12 detector in Hall B [28]. I discussed two high profile programs that would very significantly benefit from a high performance polarized positron source and accelerated beam. The first program fits well into the already developed 3D-imaging program with electron beams, where the imaginary part of the DVCS amplitude can be extracted. The program with polarized positrons enables access to the azimuthally even BH-DVCS interference terms that are directly related to the real part of the scattering amplitude. Moreover, by avoiding use of the Rosenbluth separation technique, the leading contributions to the cross sections may be separated in the full kinematical range available at the JLab 12 GeV upgrade. Even at modest polarized positron beam currents of 8nA good statistical accuracy can be achieved for charge differences and charge asymmetries. For efficient use of polarized targets higher beam currents of up to 40nA are needed to compensate for the dilution factor of ~ 0.18 inherent in the use of currently available polarized proton targets based on ammonia as target material, and to allow for a more complete DVCS and GPD program at 12 GeV. The second program requiring positron beams is the measurement of the 2-photon exchange contributions in the elastic electron-proton scattering. The measurements we outlined, if properly executed with excellent control of systematic uncertainties, should close the book on the discrepancies in the ratio of electric to magnetic form factors when measured with two different methods.

In this talk we have focussed on experiments with a large acceptance detector, which may be the only option given the low current expected for polarized positron beams of high polarization and good beam parameters. Positron currents in excess of $1\mu\text{A}$ may be required to make positron beams attractive for an experimental program with focusing, high resolution magnetic spectrometers.

Acknowledgments

I like to thank Harut Avakian for providing me with the experimental projections for the DVCS experiment, and the elastic ep scattering cross sections and rate calculations. This material is based upon work supported by the U.S. Department of Energy, Office of Science, Office of Nuclear Physics under contract DE-AC05-06OR23177.

REFERENCES

- [1] M. Diehl, Phys. Rept. **388**, 41 (2003) [hep-ph/0307382].
- [2] A. V. Belitsky and A. V. Radyushkin, Phys. Rept. **418**, 1 (2005) [hep-ph/0504030].
- [3] A. V. Belitsky, X. d. Ji and F. Yuan, Phys. Rev. D **69**, 074014 (2004) [hep-ph/0307383].
- [4] X. d. Ji, Phys. Rev. Lett. **91**, 062001 (2003) [hep-ph/0304037].
- [5] M. Burkardt, Int. J. Mod. Phys. A **18**, 173 (2003) [hep-ph/0207047].
- [6] H. S. Jo *et al.* [CLAS Collaboration], Phys. Rev. Lett. **115**, no. 21, 212003 (2015) [arXiv:1504.02009].
- [7] G. Gavalian *et al.* [CLAS Collaboration], Phys. Rev. C **80**, 035206 (2009) [arXiv:0812.2950 [hep-ex]].
- [8] F. X. Girod *et al.* [CLAS Collaboration], Phys. Rev. Lett. **100**, 162002 (2008) [arXiv:0711.4805 [hep-ex]].
- [9] C. M. Camacho *et al.* [Jefferson Lab Hall A], Phys. Rev. Lett. **97**, 262002 (2006) [nucl-ex/0607029].
- [10] S. Stepanyan *et al.* [CLAS Collaboration], Phys. Rev. Lett. **87**, 182002 (2001) [hep-ex/0107043].
- [11] S. Pisano *et al.* [CLAS Collaboration], Phys. Rev. D **91**, no. 5, 052014 (2015) [arXiv:1501.07052 [hep-ex]].
- [12] E. Seder *et al.* [CLAS Collaboration], Phys. Rev. Lett. **114**, no. 3, 032001 (2015) Addendum: [Phys. Rev. Lett. **114**, no. 8, 089901 (2015)] [arXiv:1410.6615 [hep-ex]].
- [13] S. Chen *et al.* [CLAS Collaboration], Phys. Rev. Lett. **97**, 072002 (2006) [hep-ex/0605012].
- [14] M. Guidal, H. Moutarde and M. Vanderhaeghen, Rept. Prog. Phys. **76**, 066202 (2013) [arXiv:1303.6600].
- [15] K. Kumericki and D. Mueller, arXiv:1205.6967 [hep-ph].
- [16] M. N. Rosenbluth, Phys. Rev. **79**, 615 (1950).
- [17] JLab experiment E12-06-119, F. Sabatie *et al.* (spokespersons).
- [18] M. Vanderhaeghen, P. A. M. Guichon and M. Guidal, Phys. Rev. D **60**, 094017 (1999) [hep-ph/9905372].
- [19] A. V. Belitsky, D. Mueller and A. Kirchner, Nucl. Phys. B **629**, 323 (2002) [hep-ph/0112108].
- [20] M. Diehl and S. Sapeta, Eur. Phys. J. C **41**, 515 (2005) [hep-ph/0503023].
- [21] V. Guzey and T. Teckentrup, Phys. Rev. D **79**, 017501 (2009) [arXiv:0810.3899 [hep-ph]].
- [22] V. Guzey and T. Teckentrup, Phys. Rev. D **74**, 054027 (2006) [hep-ph/0607099].
- [23] I. A. Rachek *et al.*, Phys. Rev. Lett. **114**, no. 6, 062005 (2015) [arXiv:1411.7372 [nucl-ex]].
- [24] D. Rimal *et al.* [CLAS Collaboration], Phys. Rev. C **95**, no. 6, 065201 (2017) [arXiv:1603.00315 [nucl-ex]].
- [25] D. Adikaram *et al.* [CLAS Collaboration], Phys. Rev. Lett. **114**, 062003 (2015) [arXiv:1411.6908 [nucl-ex]].
- [26] B. S. Henderson *et al.* [OLYMPUS Collaboration], Phys. Rev. Lett. **118**, no. 9, 092501 (2017) [arXiv:1611.04685 [nucl-ex]].
- [27] A. Afanasev, P. G. Blunden, D. Hasell and B. A. Raue, Prog. Part. Nucl. Phys. **95**, 245 (2017) [arXiv:1703.03874 [nucl-ex]].
- [28] V. D. Burkert, Proc. Int. Sch. Phys. Fermi **180**, 303 (2012) [arXiv:1203.2373 [nucl-ex]].